ACS Chemical Neuroscience

Research Article

pubs.acs.org/chemneuro

Discovery of *N*-Alkyl Catecholamides as Selective Phosphodiesterase-4 Inhibitors with Anti-neuroinflammation Potential Exhibiting Antidepressant-like Effects at Non-emetic Doses

Zhong-Zhen Zhou,*[,†] Yu-Fang Cheng,[†] Zheng-Qiang Zou,[†] Bing-Chen Ge,[†] Hui Yu,[†] Cang Huang,[†] Hai-Tao Wang,[†] Xue-Mei Yang,*[,‡] and Jiang-Ping Xu*[,†]

[†]Department of Neuropharmacology and Novel Drug Discovery, School of Pharmaceutical Sciences, Southern Medical University, Guangzhou 510515, China

[‡]Hygiene Detection Center, School of Public Health, Southern Medical University, Guangzhou 510515, China

Supporting Information

ABSTRACT: Depression involving neuroinflammation is one of the most common disabling and life-threatening psychiatric disorders. Phosphodiesterase 4 (PDE4) inhibitors produce potent antidepressant-like and cognition-enhancing effects. However, their clinical utility is limited by their major side effect of emesis. To obtain more selective PDE4 inhibitors with antidepressant and anti-neuroinflammation potential and less emesis, we designed and synthesized a series of *N*-alkyl catecholamides by modifying the 4-methoxybenzyl group of our hit compound, FCPE07, with an alkyl side chain. Among these compounds, 10 compounds displayed submicromolar IC_{50} values in the mid- to low-nanomolar range. Moreover, 4-difluoromethoxybenzamides **10g** and **10j**, bearing isopropyl groups, exhibited the highest PDE4 inhibitory activities, with IC_{50} values in the low-nanomolar range and with higher selectivities for PDE4 (approximately 5000-fold and 2100-fold over other PDEs, respectively). Furthermore, compound **10j** displayed anti-neuroinflammation potential, promising antidepressant-like effects, and a zero incidence rate of emesis at 0.8 mg/kg within 180 min.

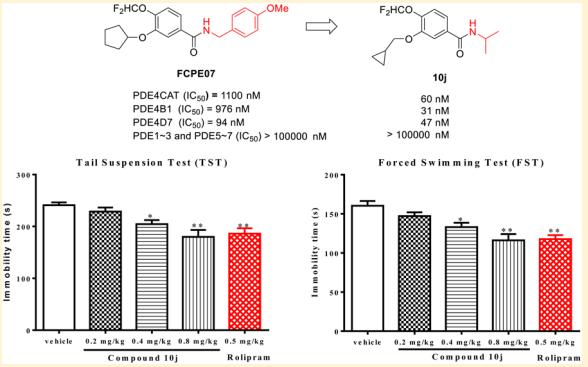

KEYWORDS: *N-Alkyl catecholamide, selective phosphodiesterase-4 inhibitors, anti-neuroinflammation, antidepressant-like effects, less side-effect, structure−activity relationships*

Depression accompanied by cognitive dysfunction is one of the most common psychiatric disorders, affecting up to 21% of the population worldwide.[1,2] Furthermore, major depressive disorder is a severe, chronic, and life-threatening illness with a lifetime prevalence of more than 10%.[3] Mounting evidence indicates that inflammatory and neurodegenerative processes play an important role in depression and that enhanced neurodegeneration in depression may be at least partly attributed to inflammation.[1,4,5] Inhibition of tumor necrosis factor-α (TNF-α),[6] cyclooxygenase-2 (COX-2),[7] and inducible nitric oxide synthase (iNOS)[5] alleviates depressive symptoms. Therefore, antidepressant agents with anti-neuroinflammatory effects are proposed to be more effective.

Phosphodiesterase 4 (PDE4), which specifically catalyzes the hydrolysis of cAMP, is highly expressed in brain regions regulating memory, anxiety, and depression.[8,9] It is composed of four genes (*PDE4A* to *PDE4D*), each with multiple transcripts that produce three protein isoforms, termed long, short, and super short.[10] Altered cAMP signal transduction is a promising mechanism underlying reduced synaptic plasticity and neuronal survival in the pathophysiology of depression.[11] This hypothesis provides a framework in which co-therapy for depression is mediated via cAMP signaling. Also, increasing evidence suggest that cAMP signaling plays a pivotal role in long-term memory-enhancing effects[12,13] and anti-inflammatory activities.[14] Additionally, genetic knockdown of PDE4B[15,16] or PDE4D[17,18] enzyme in rats produces an antidepressant phenotype. Furthermore, the inhibition of PDE4B leads to reduction of neuroinflammation by dampening microglia cytokine production,[19] while the inhibition of PDE4D has potent cognitive benefits by augmenting signaling through the cAMP/protein kinase A/cAMP response element-binding protein (CREB) pathway for memory consolidation.[20] Thus, PDE4 represents a potential therapeutic target for depression.[21]

The development of PDE4 inhibitors has primarily focused on novel anti-inflammatory therapies for asthma, chronic obstructive pulmonary disease, and atopic dermatitis for several decades. However, although a large number of PDE4 inhibitors

Received: August 28, 2016
Accepted: October 3, 2016

DOI: 10.1021/acschemneuro.6b00271
ACS Chem. Neurosci. XXXX, XXX, XXX−XXX

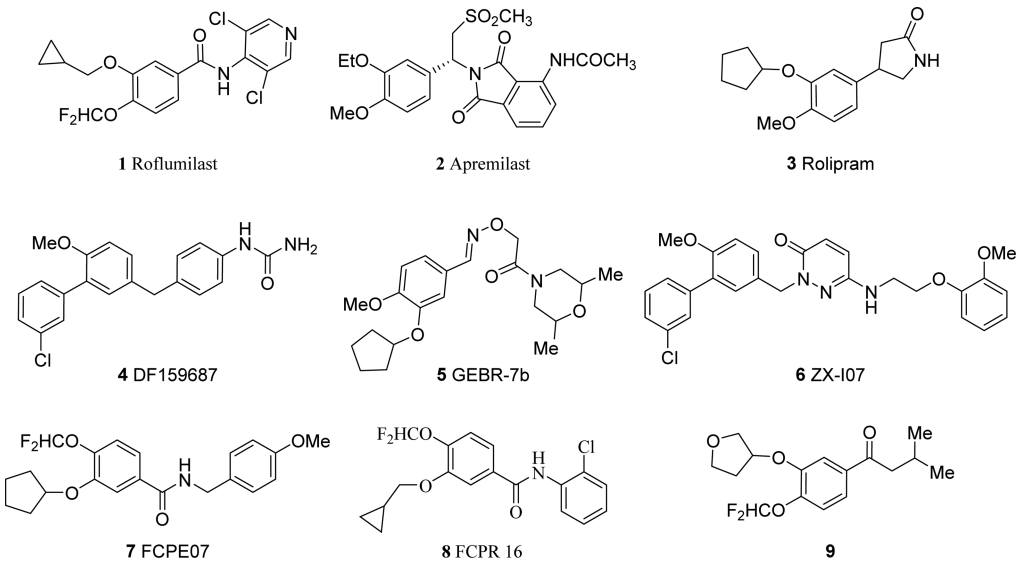

Figure 1. PDE4 inhibitors.

have been clinically evaluated, only roflumilast (**1**)[22] and apremilast (**2**)[23] (Figure 1) are currently approved. In addition, a small number of PDE4 inhibitors are used in clinical testing to target neurological diseases. For example, the first-generation PDE4 inhibitor rolipram (**3**) exhibits antidepressant activity[18,24] and memory enhancement[25−27] by elevating the concentration of intracellular cAMP. However, its side effects resulted in commercial failure of the product. Nevertheless, many PDE4D inhibitors with antidepressant activities, memory-enhancing effects, and less side effects have been identified (Figure 2),

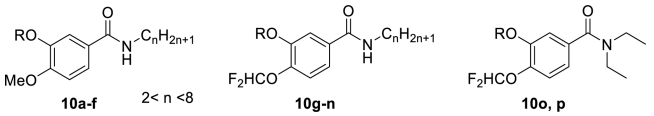

Figure 2. Structures of *N*-alkyl catecholamides (**10a−p**).

such as DF159687,[28] GEBR-7R,[29] and ZX-I07 (chlorbipram).[30] Our recent study of selective PDE4 inhibitors led to the discovery of FCPE07 (**7**),[31] which contains a short amide linker (−$CONHCH_2$−) and a 4-methoxybenzyl group; this compound is a potent and selective PDE4D inhibitor (IC_{50} = 94 nM) that exhibited a 10-fold selectivity over the PDE4B subtype and a selectivity of over 1000-fold against other PDE family members (PDE1−3 and PDE5−11). Compound FCPR16 (**8**)[32] bearing a 2-chlorophenyl group was identified as selective PDE4 inhibitor (about 1111-fold over other PDEs) with IC_{50} values in the low-nanomolar range and inhibited LPS-induced TNF-α production in microglia.

Furthermore, catechol bearing alkyl side chains also displayed good selectivity for PDE4. For example, compound **9**, with an alkyl side chain, is a selective PDE4 inhibitor with IC_{50} values in the low-nanomolar range.[33] In this paper, to obtain highly selective PDE4 inhibitors with antidepressant and anti-neuroinflammatory activities and less emesis, we synthesized small molecules by modifying the 4-methoxybenzyl group in the side chain of FCPE07 with alkyl side chains (Figure 2). The pharmacological profile, pharmacokinetics analysis, structure−activity relationships (SARs), and molecular modeling of these compounds are also described.

RESULTS AND DISCUSSION

Chemistry. *N*-Alkyl catecholamides (**10a−p**) were prepared from 4-alkoxy-3-alkoxybenzoic acids (**11a−d**) using our prior synthetic methodology,[31] as shown in Scheme 1. Acids (**11a−d**) were converted by thionyl chloride to corresponding substituted benzoyl chlorides (**12a−d**), which were subsequently reacted with the corresponding amines to prepare benzamides **10a−p** in good yields.

Enzymatic Assays. The catalytic domains of all PDE4 subtypes (PDE4A−D) exhibited a high degree of sequence

Scheme 1. Synthetic Route for Compounds 10a−p

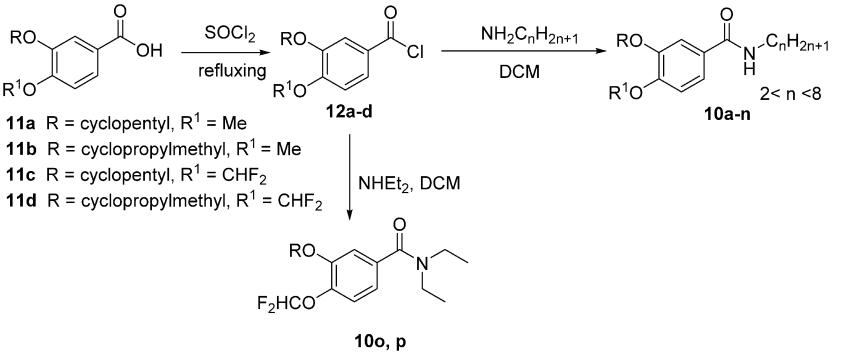

DOI: 10.1021/acschemneuro.6b00271
ACS Chem. Neurosci. XXXX, XXX, XXX−XXX

Table 1. Inhibition of PDE4CAT by Target Compounds 10a−p

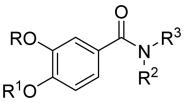

compd	R	R^1	R^2	R^3	IC_{50} (nM)[a]
10a	cyclopentyl	Me	H	*i*-Pr	170
10b	cyclopentyl	Me	H	*n*-Pr	380
10c	cyclopentyl	Me	H	*n*-Bu	1000
10d	cyclopropylmethyl	Me	H	*i*-Pr	360
10e	cyclopropylmethyl	Me	H	*n*-Pr	740
10f	cyclopropylmethyl	Me	H	*n*-Bu	1500
10g	cyclopentyl	CHF_2	H	*i*-Pr	20
10h	cyclopentyl	CHF_2	H	*n*-Pr	80
10i	cyclopentyl	CHF_2	H	*n*-Bu	300
10j	cyclopropylmethyl	CHF_2	H	*i*-Pr	60
10k	cyclopropylmethyl	CHF_2	H	*n*-Pr	70
10l	cyclopropylmethyl	CHF_2	H	*n*-Bu	290
10m	cyclopentyl	CHF_2	H	*n*-octyl	34000
10n	cyclopropylmethyl	CHF_2	H	*n*-octyl	26000
10o	cyclopentyl	CHF_2	Et	Et	2000
10p	cyclopropylmethyl	CHF_2	Et	Et	3900
FCPE07[b]	cyclopropylmethyl	CHF_2	H	4-methoxybenzyl	1100
rolipram					550

[a]Data reported represent the mean of two experiments. [b]Data for compound FCPE07 were extracted from ref 31.

conservation, with a single active-site amino acid determining the nucleotide selectivity.[34,35] Therefore, all the synthesized compounds were initially tested in duplicate on PDE4CAT (the core catalytic domains of human PDE4) according to reported protocols,[36] using rolipram as a positive control. All the compounds were tested on PDE4CAT at nine different concentrations (10^{-8} to 10^{-4} M). The IC_{50} values were determined by nonlinear regression analysis of their inhibition curves (see Table 1). Compared with rolipram and FCPE07, most *N*-alkyl catecholamides (**10a−p**) showed excellent inhibitory activities against PDE4CAT, having IC_{50} values in the mid- to low-nanomolar range. *N*-Alkyl catecholamides (**10a−p**) bearing isopropyl and *n*-propyl groups displayed higher inhibitory activities then FCPE07 and rolipram.

To obtain more information about their subtype selectivities, the most active compounds (**10g−i** and **10j−l**) were further tested in full length human PDE4A4, PDE4B1, PDE4C1, and PDE4D7, which were purchased form BPS Bioscience Inc. As shown in Table 2, the results suggest that all the screened compounds displayed higher PDE4D7 inhibitory activities than PDE4A4. Compounds **10g** and **10j**, which bear an isopropyl group, showed excellent PDE4B1 and PDE4D7 inhibitory activities, higher than those of rolipram and FCPE07.

Table 2. Inhibition (IC_{50}, nM)[a] of Four PDE4 Subtypes

compd	PDE4A4	PDE4B1	PDE4C1	PDE4D7
10g	32	10	79	21
10h	110	*b*	*b*	87
10i	397	*b*	*b*	190
10j	113	31	164	47
10k	160	*b*	*b*	122
10l	569	*b*	*b*	352
FCPE07[c]	*b*	976	*b*	94
rolipram	386	86	118	160

[a]Data represent the mean of two experiments. [b]Not tested. [c]Data for compound FCPE07 were extracted from ref 31.

PDEs exist as 11 different isozymes involved in various physiological processes. Therefore, selective inhibition of PDE4 is very important. We determined the selectivity of compounds **10g** and **10j** toward the other PDE isoforms using human PDE1A1, PDE1A, PDE2A, PDE3B, PDE5A, PDE6C, PDE7A, PDE8A1, PDE9A2, PDE10A2, and PDE11A, which were purchased form BPS Bioscience Inc. (Table 3). As shown in Table 3, compounds **10g** and **10j** displayed high PDE4 selectivity, at least 5000- and 2100-fold over other PDEs, respectively.

Structure−Activity Relationships (SAR) and Docking Study. Careful analysis of the SAR of *N*-alkyl catecholamides (**10a−p**) reveals that the substituents on the catecholic group and *N*-alkyl groups have profound effects on the inhibitory activities of the compounds. First, *N*-alkylbenzamides bearing a difluoromethoxy group (**10g−l**) always exhibit higher inhib-

Table 3. Inhibition of PDEs (PDE1−3 and PDE5−11)

	10g		**10j**	
PDEs[a]	at 10 μM[b]	IC_{50}[c] (μM)	at 10 μM[b]	IC_{50}[c] (μM)
PDE1A	3	>100	5	>100
PDE2A	12	>100	13	>100
PDE3B	6	>100	6	>100
PDE5A	23	>100	22	>100
PDE6C	11	>100	17	>100
PDE7A	3	>100	5	>100
PDE8A1	19	>100	15	>100
PDE9A2	5	>100	8	>100
PDE10A2	4	>100	8	>100
PDE11A	12	>100	14	>100

[a]All PDEs are full enzyme with N-terminal GST-tag. [b]Inhibition (%) of selected compounds at 10 μM. Data represent the mean of two experiments. [c]Data represent the mean of two experiments.

DOI: 10.1021/acschemneuro.6b00271
ACS Chem. Neurosci. XXXX, XXX, XXX−XXX

itory activities than their corresponding analogues bearing a methoxy group (**10a−f**). Second, the inhibitory activities of compounds **10a−p** against PDE4CAT, PDE4A, and PDE4D were consistently improved by shortening the chain length. Among these compounds, 4-difluoromethoxybenzamides bearing a long alkyl chain (e.g., **10m** and **10n**) displayed substantially weaker inhibitory activities. However, 4-difluoromethoxybenzamides bearing propyl groups (such as *n*-Pr and *i*-Pr) exhibited the highest PDE4 inhibitory activities, with IC_{50} values in the low-nanomolar range. Third, the configuration of the alkyl groups on the catechol-based amides affects their inhibitory activities. For example, all benzamides bearing an isopropyl group (such as **10a**, **10d**, **10g**, and **10j**) showed higher inhibitory activities than their corresponding analogues with an *n*-propyl group (such as **10b**, **10e**, **10h**, and **10k**). Finally, *N*,*N*-dialkyl catecholamides displayed very weak inhibitory activities (e.g., **10o** and **10p**). The SAR results for the *N*-alkyl catecholamides (**10a−p**) reveal that the activities decrease in the following order: isopropyl > *n*-propyl > *n*-butyl > diethyl > *n*-octyl.

To gain insight into the SARs and the observed selectivity, we studied the binding of the synthetic inhibitors in PDE4D (PDB code 3G4K[28]). The catechol motif in catecholic PDE4 inhibitors is known to accept a double hydrogen bond from the carboxamide group of a glutamine residue at the back of the PDE4 catalytic site.[34,37,38] As shown in Figure 3, docking of

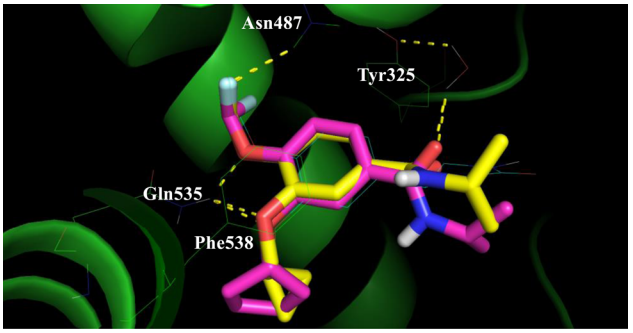

Figure 3. Potential binding configuration of **10g** and **10j** in the active site of PDE4D. The C atoms in **10g** and **10j** are colored in magenta and yellow, respectively; the total docking scores of **10g** and **10j** are 9.3383 and 9.1722, respectively. The native ligand, rolipram (total docking score = 9.018), is shown in the thin wire model, and C atoms are colored in cyan. The H-bonds between each ligand and the active-site amino acids are shown in yellow.

compounds **10g** and **10j** into PDE4D showed very similar binding configurations and reasonably good overlap with the native ligand. In the active site of PDE4D, the catechol moieties in **10g** and **10j** were predicted to occupy the pocket of the catechol moiety in rolipram, with subtle variations, and interact with the binding site by hydrogen bonding with the NH_2 group of the Gln535 residue and by π-stacking with Phe538. Meanwhile, the 4-difluoromethyl group is in position to form a hydrogen bond with Asn487. Thus, the improvement in activity of the *N*-alkylbenzamides (**10g−l**) bearing a difluoromethoxy group could be attributed to the extra H-bond of the 4-difluoromethyl group with the Asn487 residue. In addition, the linker region ($CONHCH_2$) developed an additional hydrogen bond with a conserved water molecule, which extends to Tyr325. Similar water bridges were also observed in other docking studies of selective PDE4 inhibitors.[31,39,40] For example, FCPE07 forms two water bridges in contact with the Ser374 and Ser521 residues.[31]

Anti-neuroinflammatory Activity in Microglial Cells. Previous research[41−43] suggests that inhibition of the inflammatory cytokine tumor necrosis factor (TNF) in depressed patients with increased inflammation can be associated with decreased depressive symptoms. Also, the pro-inflammatory toll receptor TNF-α pathway in monocytes, macrophages, and microglial cells (BV-2) is regulated by PDE4.[4,44] Here lipopolysaccharide (LPS) was used to induce an inflammatory effect in microglia BV-2 cells. To determine the effect of **10j** on BV-2 activation, Western blot analysis was performed to assess the protein levels of TNF-α, iNOS, and COX-2 in response to LPS.

First, microglial cells were treated with different concentrations of **10j** (5, 20, and 80 μM, dimethyl sulfoxide (DMSO) final concentration = 0.1%) for 1 h and then incubated with LPS (1 μg/mL) for 24 h. Prior to studying the impact of **10j** on LPS-induced neuroinflammation, we examined the potential toxic effects of **10j** on BV-2 microglial cells. Our data showed that individual treatments with **10j** and LPS did not produce any signs of toxicity at the selected concentrations. We also found that **10j** alone at a dose of 80 μM had no toxic effects on BV-2 microglial cells (Figure 4).

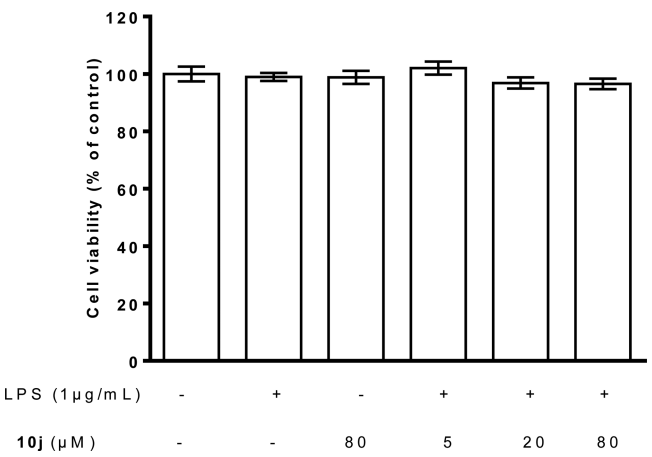

Figure 4. Cell viability of BV-2 cells treated with **10j**. Cells were incubated with indicated concentrations of **10j** for 1 h before incubation with LPS (1 μg/mL) for 24 h. Cell viability was evaluated using the MTT assay. Results are shown as percentages of the control sample, which was set as 100%. Values are means ± standard error of mean (SEM) from three independent experiments.

We then investigated the effect of compound **10j** on the expression of pro-inflammatory factors in BV-2 cells. As shown in Figure 5, compound **10j** alone had no effect on the production of TNF-α, iNOS, and COX-2 in microglia at a concentration of 80 μM. Stimulation of microglia with LPS alone led to significant increases in TNF-α, iNOS, and COX-2 levels 24 h after treatment. Interestingly, compound **10j** was able to suppress LPS-induced TNF-α, iNOS, and COX-2 production in a concentration-dependent manner (Figure 5B,C,D). Compound **10j** inhibited LPS-induced TNF-α, iNOS, and COX-2 production in microglia ($p < 0.01$) at a concentration of 80 μM. Furthermore, microglia cells treated with **10j** at a concentration of 5 μM also inhibited LPS-induced TNF-α production (Figure 5B,C,D). These data demonstrate that PDE4 inhibitor compound **10j** can effectively inhibit LPS-

DOI: 10.1021/acschemneuro.6b00271
ACS Chem. Neurosci. XXXX, XXX, XXX−XXX

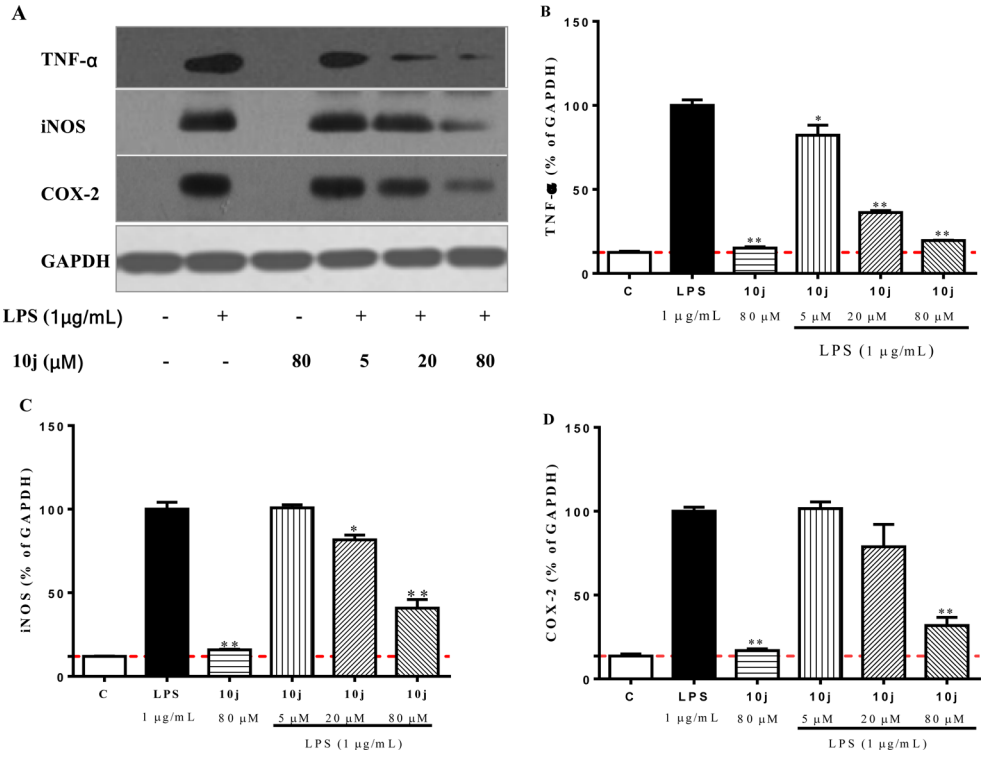

Figure 5. Compound **10j** inhibited LPS-induced production of pro-inflammatory cytokines in microglial cells. Quantitative analysis of TNF-α (B), iNOS (C), and COX-2 (D) in microglia treated with compound **10j** and LPS. Data are represented as mean ± SEM from three independent experiments; *p < 0.05, **p < 0.01 versus LPS alone group.

induced TNF-α secretion, iNOS generation, and COX-2 expression.

Antidepressant Behavioral Evaluation *in Vivo*. Based on the fact that neuroinflammation is involved in the pathology of depression and based on our *in vitro* data presented above, compound **10j** was selected for further *in vivo* experiments to evaluate its antidepressant effects. The pharmacological action of selective PDE4 inhibitor **10j** was evaluated using the tail suspension test (TST) and forced swimming test (FST), which were performed for 6 min as previously described;[30,45] rolipram was used as a positive control. In two mouse models, compound **10j** was administered by intraperitoneal injection at 0.2, 0.4, and 0.8 mg/kg. Antidepressant behavior was indicated by a decrease in the immobility time of the animals. The results are shown in Figure 6.

To determine whether compound **10j** indeed exhibited antidepressant-like effects, we investigated the central stimulation. We measured the spontaneous locomotor activity of mice after drug administration with the open field test over a 5 min testing period. As shown in Figure 6A,B, statistical analysis by one-way ANOVA showed that compound **10j** and rolipram did not produce any significant differences in rearing and movement numbers (crossings) when compared with the saline-treated group. Next, acute effects of **10j** on the immobility time of C57BL/6 mice in the TST and FST during the total 6 min observation period were analyzed. In the TST and FST, immobility is defined as the absence of all except respiratory movement of the mouse. As shown in Figure 6C,D, our results indicated that pretreatment with **10j** decreased the duration of immobility at all testing doses in the TST and FST, with significant decreases in immobility time observed at the doses of 0.4 mg/kg (p < 0.05) and 0.8 mg/kg (p < 0.01) compared with the vehicle treatment group.

Emetic Potential of Compound 10j. It is well-known that many PDE4 inhibitors have not been brought to market because of issues related to tolerability, such as emesis. Therefore, in order to investigate its emetic properties, we profiled our compound **10j**, which displayed anti-neuroinflammation potential and promising antidepressant-like effects, in the ketamine/xylazine test, which has been proposed as a behavioral correlate of emesis in mice.[28,46,47] As shown in Figure 7, rolipram reduces the duration of xylazine/ketamine-induced anesthesia in the ketamine/xylazine test at an antidepressant-like dose. However, compound **10j** does not reduce the duration of ketamine/xylazine-induced anesthesia up to 1.5 mg/kg, which is a higher dose than that which results in maximal antidepressant effects in mice.

To further investigate the topic of emesis, we profiled compound **10j** for its emetic activity in beagle dogs (Table 4), which have been used for preclinical testing of novel antinausea compounds and for assessing the emetic liability of novel medicines within the pharmaceutical industry.[28,30,48] Beagle dogs were dosed with compound **10j** and rolipram by oral administration. Emetic activity was expressed as the incidence rate, that is, the number of animals showing emesis per number of animals (n = 3 or 4) tested at the respective dose within 180 min. As shown in Table 4, the incidence rate of emesis of rolipram is 100% at 0.8 mg/kg, and the latency of emesis is much shorter (35 ± 1.5 min). However, the incidence rate of emesis of compound **10j** is zero at 0.8 mg/kg within 180 min.

Pharmacokinetics Analysis of Compound 10j. In addition, intravenous pharmacokinetics and oral bioavailability of compound **10j** were evaluated in mice. As shown in Table 5, compound **10j** showed a high clearance and a relatively high volume of distribution in mice after intravenous (iv) treatment at 1 mg/kg. The average time spent between infusion and

DOI: 10.1021/acschemneuro.6b00271
ACS Chem. Neurosci. XXXX, XXX, XXX−XXX

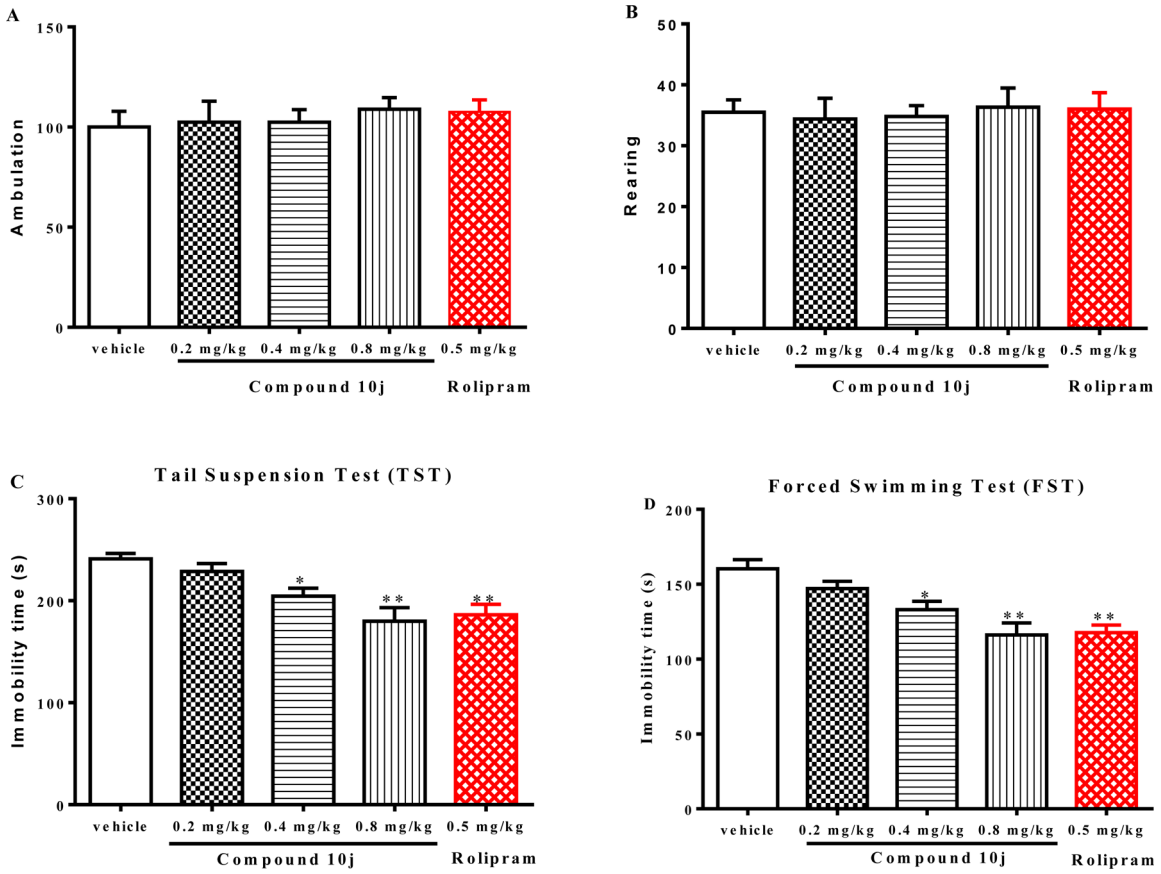

Figure 6. Antidepressant behavioral evaluation of compound **10j** *in vivo* at graded doses (dose range 0.2 to 0.8 mg/kg) using DMSO (5%) in saline (0.9%) and rolipram (0.5 mg/kg) as the vehicle and positive control, respectively. (A) Ambulation times and (B) rearing times represent the acute effects of locomotor activity in C57BL/6 mice during the 5 min testing period in the open field test. (C) TST and (D) FST show the acute effects of **10j** on immobility time during the total 6 min testing period in C57BL/6 mice. Results are represented as mean ± SEM (n = 6–9); *p < 0.05 and **p < 0.01 versus vehicle-treated group.

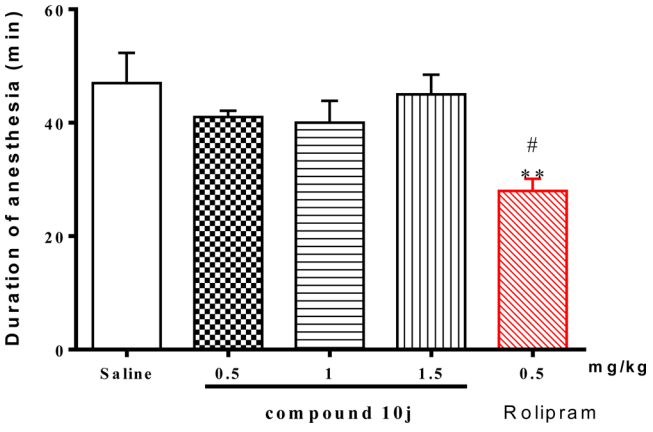

Figure 7. Effects of compound **10j** and rolipram on the duration of anesthesia (min) induced by the combination of xylazine (10 mg/kg) and ketamine (70 mg/kg) in C57BL/6 mice. Each column represents mean ± SEM (n = 6–8); **p < 0.01 versus vehicle-treated group; #p < 0.05 versus compound **10j** (0.5 mg/kg).

elimination (mean residence time, MRT) was about 34 min, whereas the elimination half-time ($T_{1/2}$) was 68 min.

After oral (po) administration at 5 mg/kg, the profile of compound **10j** showed a rapid absorption (T_{max} = 11.5 min, time to reach C_{max}) and long MRT = 326 min, but low oral bioavailability of 1.23%, whereas the elimination half-time ($T_{1/2}$) was about 211 min (Table 5, bottom panel). We noticed that compound **10j** displayed low bioavailability;, however, the anti-neuroinflammatory potential and antidepressant-like effect of compound **10j** have been verified in our studies, which provides the possibility that the pharmacological effects of **10j** will be enhanced under conditions of improved bioavailability. Hence, further studies are required for the pharmaceutical form of compound **10j** to improve the bioavailability.

Table 4. Effects of Compound 10j on Emesis in Beagle Dogs

compd	dose (mg/kg)	incidence rate of emesis (%)	latency of emesis[a] (min)
10j	0.8	0 (0/4)	>180
rolipram	0.8	100 (3/3)	35 ± 1.5
vehicle		0 (0/4)	>180

[a]Values are expressed as mean ± SD.

CONCLUSIONS

The structural modification of our hit compound FCPE07 yielded novel catecholamides bearing *N*-alkyl side chains, which selectively inhibited PDE4 enzymes with increased potency. Reports suggest that PDE4B is the main PDE4 isoform mediating TNF-α release,[49] while the PDE4D isoform is associated with depression and memory.[17,20,50] Compounds **10g** and **10j** effectively inhibited the activity of PDE4B1 and PDE4D7 enzymes at low-nanomolar IC_{50} values, with

DOI: 10.1021/acschemneuro.6b00271
ACS Chem. Neurosci. XXXX, XXX, XXX−XXX

Table 5. Pharmacokinetic Profile of PDE4 Inhibitor 10j in Mice/Rats

	CL ($L\ h^{-1}\ kg^{-1}$)	V_{ss} ($L\ kg^{-1}$)	$MRT_{(0-\infty)}$ (h)	$AUC_{(0-t)}$ (ng·h/L)	$AUC_{(0-\infty)}$ (ng·h/L)	C_{max} (ng/L)	$T_{1/2}$ (h)	T_{max} (h)
route iv (1 mg/kg)	2.70 ± 0.16	4.38 ± 1.06	0.57 ± 0.09	367 ± 22.72	371.29 ± 22.73	857.77 ± 36.27	1.13 ± 0.28	0.083 ± 0.00
	$MRT_{(0-\infty)}$ (h)	$AUC_{(0-t)}$ (ng·h/L)	$AUC_{(0-\infty)}$ (ng·h/L)	C_{max} (ng/L)	$T_{1/2}$ (h)	T_{max} (h)	F (%)	
route po (5 mg/kg)	5.44 ± 1.76	6.82 ± 1.53	22.81 ± 5.34	5.60 ± 1.42	3.69 ± 1.17	0.194 ± 0.096	1.23 ± 0.29	

selectivities of at least 5000- and 2100-fold over other PDEs, respectively. In addition, compound **10j** inhibited LPS-induced TNF-α, iNOS, and COX-2 production in microglia. Further, compound **10j** significantly decreased immobility duration when administered orally at doses of 0.4 and 0.8 mg/kg in two tests (TST and FST). More interestingly, compound **10j** did not cause emesis during the 180 min observation period at 0.8 mg/kg.

In pharmacokinetics studies, compound **10j** showed a long half-life and a rapid clearance and therefore a large volume of distribution, but a low oral bioavailability in mice. Pharmacokinetic properties still need to be improved; however, considering its attractive anti-neuroinflammatory potential and antidepressant-like effects, compound **10j** represents an important lead compound for further refinements and proof-of-concept studies.

METHODS

Chemistry. ESI spectra were measured on a Waters UPLC/Quattro Premier XE mass spectrometer. ^{1}H and ^{13}C NMR spectra were recorded in $CDCl_3$ or d_6-DMSO using a Varian Mercury 400 spectrometer and TMS as an internal reference. Elemental analyses were carried out on a Vario ELIII CHNSO elemental analyzer. Rolipram was purchased from Sigma (St. Louis, MO, USA). All the other chemicals were of analytical grade and used without further purification.

*General Protocol for Preparation of Compounds **11a–d**.*[31] We used the procedure already reported for 4-methoxy-3-alkoxybenzoic acids (**11a,b**) and 4-difluoromethoxy-3-hydroxybenzaldehyde (**11c,d**).

*General Protocol for Preparation of Compounds **10a–p**.* Excess thionyl chloride (5 mL) was added to the intermediate alkoxybenzoic acid (0.5 mmol). The reaction mixture was then stirred at 60−80 °C for 3 h. The excess thionyl chloride was evaporated under reduced pressure to give a corresponding alkoxybenzoyl chloride as crude yellow oil, which was used in all the following reactions without further purification.

Suitable amine (0.5 mmol) and anhydrous triethylamine (1 mmol) were dissolved in dry CH_2Cl_2 (5 mL). The mixture was cooled on ice and treated dropwise (during 5 min) with a solution of previously prepared alkoxybenzoyl chloride in dry CH_2Cl_2 (2 mL) at 0 °C. The reaction mixture was stirred at room temperature for 3 h and monitored by TLC. Then, the reaction mixture was concentrated under reduced pressure, and the residue was chromatographed using a mixture of petroleum ether and acetone (v/v = 20:1) to give target compounds.

All the compounds were fully characterized by LC-MS and NMR (^{1}H and ^{13}C) (see Supporting Information).

*N-Isopropyl-3-(cyclopentyloxy)-4-methoxybenzamide (**10a**).* Yield: 64%. ^{1}H NMR (400 MHz, $CDCl_3$) δ 7.40 (s, 1H), 7.21 (d, J = 8.3 Hz, 1H), 6.84 (d, J = 8.3 Hz, 1H), 5.84 (d, J = 6 Hz, 1H), 4.90−4.77 (m, 1H), 4.31−4.22 (m, 1H), 3.88 (s, 3H), 2.03−1.93 (m, 2H), 1.92−1.77 (m, 4H), 1.63−1.56 (m, 2H), 1.25 (s, 3H), 1.27 (s, 3H). ^{13}C NMR (101 MHz, $CDCl_3$) δ 166.38, 152.76, 147.79, 127.69, 118.99, 114.28, 110.99, 80.78, 56.13, 41.88, 32.83, 24.05, 22.94. ESI-MS (m/z): 300.7 ($[M + Na]^+$), 278.7 ($[M + H]^+$). Anal. Calcd for $C_{16}H_{23}NO_3$: C, 69.29; H, 8.36; N, 5.05. Found: C, 69.01; H, 8.09; N, 5.29.

*N-Propyl-3-(cyclopentyloxy)-4-methoxybenzamide (**10b**).* Yield: 95%. ^{1}H NMR (400 MHz, $CDCl_3$) δ 7.40 (d, J = 2.0 Hz, 1H), 7.23 (dd, J = 8.3, 2.1 Hz, 1H), 6.84 (d, J = 8.4 Hz, 1H), 6.06 (s, 1H), 4.88−4.83 (m, 1H), 3.88 (s, 3H), 3.44−3.37 (m, 2H), 1.98−1.81 (m, 6H), 1.68−1.59 (m, 4H), 0.99 (t, J = 7.4 Hz, 3H). ^{13}C NMR (100 MHz, $CDCl_3$) δ 167.22, 152.79, 147.80, 127.60, 119.06, 114.25, 111.07, 80.77, 56.13, 41.79, 32.83, 24.05, 23.04, 11.46. ESI-MS (m/z): 316.9 ($[M + K]^+$), 301.0 ($[M + Na]^+$), 278.9 ($[M + H]^+$). Anal. Calcd for $C_{16}H_{23}NO_3$: C, 69.29; H, 8.36;N, 5.05. Found: C, 68.95; H, 8.07; N, 5.23.

*N-Butyl-3-(cyclopentyloxy)-4-methoxybenzamide (**10c**).* Yield: 55%. ^{1}H NMR (400 MHz, $CDCl_3$) δ 7.40 (d, J = 1.8 Hz, 1H), 7.23 (dd, J = 8.3, 1.9 Hz, 1H), 6.84 (d, J = 8.4 Hz, 1H), 6.06 (s, 1H), 4.90−4.80 (m, 1H), 3.88 (s, 3H), 3.48−3.40 (m, 2H), 2.03−1.77 (m, 6H), 1.66−1.54 (m, 4H), 1.47−1.36 (m, 2H), 0.96 (t, J = 7.3 Hz, 3H). ^{13}C NMR (101 MHz, $CDCl_3$) δ 167.17, 152.79, 147.80, 127.61, 119.07, 114.28, 111.09, 80.78, 56.13, 39.83, 32.78, 31.94, 24.04, 20.20, 13.79. ESI-MS (m/z): 314.7 ($[M + Na]^+$), 292.7 ($[M + H]^+$). Anal. Calcd for $C_{17}H_{25}NO_3$: C, 70.07; H, 8.65; N, 4.81. Found: C, 69.89; H, 8.47; N, 4.69.

*N-Isopropyl-3-(cyclopropylmethoxy)-4-methoxybenzamide (**10d**).* Yield: 70%. ^{1}H NMR (400 MHz, $CDCl_3$) δ 7.39 (d, J = 1.5 Hz, 1H), 7.23 (dd, J = 8.4, 1.5 Hz, 1H), 6.85 (d, J = 8.3 Hz, 1H), 5.82 (d, J = 5.6 Hz, 1H), 4.32−4.22 (m, 1H), 3.92−3.89 (m, 4H), 1.41−1.31 (m, 2H), 1.26 (s, 3H), 1.25(s, 3H), 0.70−0.61 (m, 2H), 0.41−0.32 (m, 2H). ^{13}C NMR (101 MHz, $CDCl_3$) δ 166.30, 152.22, 148.59, 127.69, 119.25, 112.82, 110.76, 74.23, 56.10, 41.90, 22.94, 10.28, 3.42. ESI-MS (m/z): 286.6 ($[M + Na]^+$), 264.7 ($[M + H]^+$). Anal. Calcd for $C_{15}H_{21}NO_3$: C, 68.42; H, 8.04; N, 5.32. Found: C, 68.34; H, 8.32; N, 5.09.

*N-Propyl-3-(cyclopropylmethoxy)-4-methoxybenzamide (**10e**).* Yield: 52%. ^{1}H NMR (400 MHz, $CDCl_3$) δ 7.40 (d, J = 2.0 Hz, 1H), 7.24−7.26 (m, 1H), 6.85 (d, J = 8.4 Hz, 1H), 6.06 (s, 1H), 3.92−3.90 (m, 5H, CH_3O+CH_2O), 3.40 (dd, J = 13.4 Hz, 7.0 Hz, m, 2H), 1.68−1.58 (m, 2H), 1.36−1.31 (m, 1H), 0.98 (t, J = 7.4 Hz, 3H), 0.67−0.62 (m, 2H), 0.36 (dd, J = 10.4 Hz, 4.8 Hz, 2H). ^{13}C NMR (101 MHz, $CDCl_3$) δ 167.14, 152.24, 148.60, 127.57, 119.27, 112.81, 110.80, 74.21, 56.10, 41.80, 23.04, 11.45, 10.27, 3.43. ^{13}C NMR (100 MHz, $CDCl_3$) δ 166.1, 151.2, 147.6, 126.5, 118.2, 111.8, 109.8, 73.2, 55.1, 40.8, 22.1, 10.4, 9.2, 2.4. ESI-MS (m/z): 264.6 ($[M + H]^+$). Anal. Calcd for $C_{15}H_{21}NO_3$: C, 68.42; H, 8.04; N, 5.32. Found: C, 68.23; H, 8.23; N, 5.01.

*N-Butyl-3-(cyclopropylmethoxy)-4-methoxybenzamide (**10f**).* Yield: 51%. ^{1}H NMR (400 MHz, $CDCl_3$) δ 7.40 (d, J = 2.0 Hz, 1H), 7.25 (dd, J = 8.4, 2.0 Hz, 1H), 6.86 (d, J = 8.4 Hz, 1H), 6.04 (s, 1H), 3.91−3.89 (m, 5H), 3.46−3.41(m, 2H), 1.61−1.58 (m, 2H), 1.44−1.38 (m, 2H), 1.35−1.29 (m, 1H), 0.96 (t, J = 7.4 Hz, 3H), 0.69−0.61 (m, 2H), 0.40−0.32 (m, 2H). ^{13}C NMR (101 MHz, $CDCl_3$) δ 167.10, 152.24, 148.60, 127.57, 119.27, 112.82, 110.80, 74.22, 56.10, 39.83, 31.89, 20.20, 13.79, 10.27, 3.42. ESI-MS (m/z): 278.6 ($[M + H]^+$). Anal. Calcd for $C_{16}H_{23}NO_3$: C, 69.29; H, 8.36; N, 5.05. Found: C, 69.40; H, 8.67; N, 4.94.

*N-Isopropyl-3-(cyclopentyloxy)-4-(difluoromethoxy)-benzamide (**10g**).* Yield: 74% ^{1}H NMR (400 MHz, $CDCl_3$) δ 7.50 (s, 1H), 7.16−7.12 (m, 2H), 6.58 (t, J = 75.4 Hz, 1H), 5.87 (d, J = 6.0 Hz, 1H), 4.91−4.88 (m, 1H), 4.31−4.22 (m, 1H), 1.97−1.89 (m, 4H), 1.85−1.76 (m, 2H), 1.68−1.63 (m, 2H), 1.27 (s, 3H), 1.26 (s, 3H). ^{13}C NMR (101 MHz, $CDCl_3$) δ 165.81, 149.87, 143.20, 133.48, 122.33, 118.62 ($-CHF_2$), 118.15, 116.03 ($-CHF_2$), 114.81, 113.45 ($-CHF_2$), 81.03, 42.15, 32.81, 23.88, 22.84. ESI-MS (m/z): 336.9 ($[M + Na]^+$),

DOI: 10.1021/acschemneuro.6b00271
ACS Chem. Neurosci. XXXX, XXX, XXX−XXX

314.9 ([M + H]$^+$). Anal. Calcd for $C_{16}H_{21}F_2NO_3$: C, 61.33; H, 6.76; N, 4.47. Found: C, 61.59; H, 6.70; N, 4.62.

*N-Propyl-3-(cyclopentyloxy)-4-difluoromethoxybenzamide (**10h**).* Yield: 83% ^{1}H NMR (400 MHz, $CDCl_3$) δ 7.50 (s, 1H), 7.18−7.13 (m, 2H), 6.58 (t, J = 75.2 Hz, CHF_2, 1H), 6.09 (s, 1H), 4.91−4.87 (m, 1H), 3.44−3.38 (m, 2H), 2.00−1.78 (m, 6H), 1.67−1.59 (m, 4H), 0.99 (t, J = 7.4 Hz, 3H). ^{13}C NMR (101 MHz, $CDCl_3$) δ 166.61, 149.88, 143.17, 133.37, 122.38, 118.61 (−CHF_2), 118.16, 116.02 (−CHF_2), 114.76, 113.44 (−CHF_2), 81.01, 41.92, 32.80, 23.88, 22.95, 11.43. ESI-MS (m/z): 336.7 ([M + Na]$^+$), 314.7 ([M + H]$^+$). Anal. Calcd for $C_{16}H_{21}F_2NO_3$: C, 61.33; H, 6.76; N, 4.47. Found: C, 61.57; H, 6.92; N, 4.53.

*N-Butyl-3-(cyclopentyloxy)-4-difluoromethoxybenzamide (**10i**).* Yield: 75%. ^{1}H NMR (400 MHz, $CDCl_3$) δ 7.50 (s, 1H), 7.17−7.13 (m, 2H), 6.58 (t, J = 75.2 Hz,1H), 6.06 (s, 1H), 4.91−4.87 (m, 1H), 3.47−3.42 (m, 2H), 2.01−1.86 (m, 4H), 1.86−1.75 (m, 2H), 1.68−1.62 (m, 2H), 1.61−1.56 (m, 2H), 1.46−1.37 (m, 2H), 0.96 (t, J = 7.2 Hz, 3H). ^{13}C NMR (101 MHz, $CDCl_3$) δ 166.57, 149.88, 143.20, 133.37, 122.38, 118.61 (−CHF_2), 118.14, 116.02 (−CHF_2), 114.76, 113.44 (−CHF_2), 81.00, 39.96, 32.80, 31.78, 23.87, 20.18, 13.77, 0.00. ESI-MS (m/z): 350.7 ([M + Na]$^+$), 328.7 ([M + H]$^+$). Anal. Calcd for $C_{17}H_{23}F_2NO_3$: C, 62.37; H, 7.08; N, 4.28. Found: C, 62.40; H, 6.80; N, 4.41.

*N-Isopropyl-3-(cyclopropylmethoxy)-4-difluoromethoxy benzamide (**10j**).* Yield: 82%. ^{1}H NMR (400 MHz, $CDCl_3$) δ 7.47 (d, J = 0.4 Hz, 1H), 7.20−7.15 (m, 2H), 6.68 (t, J = 75.2 Hz,1H), 5.88 (d, J = 6.0 Hz, 1H), 4.31−4.21 (m, 1H), 3.93 (d, J = 6.8 Hz, 2H), 1.33−1.30(m 1H), 1.27 (s, 3H), 1.25 (s, 3H), 0.68−0.62 (m, 2H), 0.38−0.34 (m, 2H). ^{13}C NMR (101 MHz, $CDCl_3$) δ 165.68, 150.62, 142.60, 133.41, 122.05, 118.58 (−CHF_2), 118.47, 115.88 (−CHF_2), 113.80, 113.29 (−CHF_2), 74.09, 42.12, 22.81, 10.06, 3.23. ESI-MS (m/z): 322.9 ([M + Na]$^+$), 300.9 ([M + H]$^+$). Anal. Calcd for $C_{15}H_{19}F_2NO_3$: C, 60.19; H, 6.40; N, 4.68. Found: C, 60.46; H, 6.64; N, 4.83.

*N-Propyl-3-(cyclopropylmethoxy)-4-difluoromethoxybenzamide (**10k**).* Yield: 83%. ^{1}H NMR (400 MHz, $CDCl_3$) δ 7.48 (d, J = 1.6 Hz, 1H), 7.21−7.15 (m, 2H), 6.68 (t, J = 75.2 Hz,1H), 6.11 (s, 1H), 3.93 (d, J = 6.8 Hz, 2H), 3.43−3.38 (m, 2H), 1.68−1.59 (m, 2H), 1.32−1.28 (m, 1H), 0.99 (t, J = 7.6 Hz, 3H), 0.68−0.63 (m, 2H), 0.38−0.34 (m, 2H). ^{13}C NMR (101 MHz, $CDCl_3$) δ 166.56, 150.63, 142.63, 133.27, 122.08, 118.62, 118.47, 115.88, 113.80, 113.29, 74.08, 41.91, 22.91, 11.43, 10.06, 3.23. ESI-MS (m/z): 322.8 ([M + Na]$^+$). Anal. Calcd for $C_{15}H_{19}F_2NO_3$: C, 60.19; H, 6.40; N, 4.68. Found: C, 60.38; H, 6.58; N, 4.87.

*N-Butyl-3-(cyclopropylmethoxy)-4-(difluoromethoxy)benzamide (**10l**).* Yield: 73%. ^{1}H NMR (400 MHz, $CDCl_3$) δ 7.48 (d, J = 1.6 Hz, 1H), 7.21−7.15 (m, 2H), 6.68 (t, J = 75.2 Hz,1H), 6.09 (s, 1H), 3.93 (d, J = 6.8 Hz, 2H), 3.47−3.41 (m, 2H), 1.63−1.56 (m, 2H), 1.46−1.36 (m, 2H), 1.33−1.26 (m, 1H), 0.96 (t, J = 7.4 Hz, 3H), 0.69−0.61 (m, 2H), 0.38−0.33 (m, 2H). ^{13}C NMR (101 MHz, $CDCl_3$) δ 166.55, 150.62, 142.64, 133.23, 122.07, 118.63 (−CHF_2), 118.47, 115.88 (−CHF_2), 113.80, 113.29 (−CHF_2), 74.08, 39.98, 31.72, 20.16, 13.77, 10.06, 3.23. Negative ESI-MS(m/z): 312.8 ([M − H]$^-$). Anal. Calcd for $C_{16}H_{21}F_2NO_3$: C, 61.33; H, 6.76; N, 4.47. Found: C, 61.49; H, 6.95; N, 4.59.

*N-Octyl-3-(cyclopentyloxy)-4-difluoromethoxybenzamide (**10m**).* Yield: 65%. ^{1}H NMR (400 MHz, $CDCl_3$) δ 7.53−7.47 (m, 1H), 7.18−7.11 (m, 2H), 6.58 (t, J = 75.3 Hz, 1H), 6.06 (s, 1H), 4.93−4.85 (m, 1H), 3.51−3.33 (m, 2H), 1.98−1.77 (m, 6H), 1.70−1.55 (m, 4H), 1.41−1.26 (m, 10H), 0.88 (t, J = 6.9 Hz, 3H). ^{13}C NMR (101 MHz, $CDCl_3$) δ 166.58, 149.80, 143.13, 143.10, 143.07, 133.30, 122.35, 118.58 (−CHF_2), 118.17, 116.00 (−CHF_2), 114.66, 113.42 (−CHF_2), 80.90, 40.28, 32.77, 31.80, 29.67, 29.30, 29.22, 27.03, 23.87, 22.65, 14.09. ESI-MS (m/z):406.5 ([M + Na]$^+$),384.5 ([M + H]$^+$). Anal. Calcd for $C_{21}H_{31}F_2NO_3$: C, 65.77; H, 8.15; N, 3.65. Found: C, 65.49; H, 8.01; N, 3.34.

*N-Octyl-3-(cyclopropylmethoxy)-4-difluoromethoxybenzamide (**10n**).* Yield: 76%. ^{1}H NMR (400 MHz, $CDCl_3$) δ 7.48 (d, J = 1.4 Hz, 1H), 7.21−7.14 (m, 2H), 6.68 (t, J = 75.2 Hz, 1H), 6.08 (s, 1H), 3.93 (d, J = 6.9 Hz, 2H), 3.47−3.40 (m, 2H), 1.65−1.56 (m, 2H), 1.42−1.26 (m, 11H), 0.88 (t, J = 6.9 Hz, 3H), 0.68−0.62 (m, 2H), 0.38−0.33 (m, 2H). ^{13}C NMR (101 MHz, $CDCl_3$) δ 166.54, 150.63, 142.68, 142.64, 142.61, 133.22, 122.09, 118.64, 118.48 (−CHF_2), 115.89 (−CHF_2), 113.85, 113.30 (−CHF_2), 74.10, 40.32, 31.80, 29.66, 29.29, 29.21, 27.02, 22.65, 14.09, 10.06, 3.25. Negative ESI-MS (m/z): 368.6 ([M − H]$^-$). Anal. Calcd for $C_{20}H_{29}F_2NO_3$: C, 65.02; H, 7.91; N, 3.79. Found: C, 64.88; H, 7.73; N, 3.67.

*N,N-Diethyl-3-cyclopentyloxy-4-difluoromethoxybenzamide (**10o**).* Yield: 87%. ^{1}H NMR (400 MHz, $CDCl_3$) δ 7.15 (d, J = 8.4 Hz, 1H), 6.98 (d, J = 2.0 Hz, 1H), 6.89 (dd, J = 8.0, 1.8 Hz, 1H), 6.54 (t, J = 75.2 Hz, 1H), 4.84−4.79 (m, 1H), 3.54−3.29 (m, 4H), 1.93−1.84 (m, 4H), 1.84−1.77 (m, 2H), 1.69−1.60 (m, 2H), 1.19 (s, 6H). ^{13}C NMR (101 MHz, $CDCl_3$) δ 170.39, 149.69, 141.41, 135.41, 122.75, 118.77 (−CHF_2), 118.60, 116.19 (−CHF_2), 113.61 (−CHF_2), 113.54, 80.83, 32.80, 23.87. ESI-MS (m/z): 350.9 ([M + Na]$^+$), 329.0 ([M + H]$^+$). Anal. Calcd for $C_{17}H_{23}F_2NO_3$: C, 62.37; H, 7.08; N, 4.28. Found: C, 62.43; H, 7.15; N, 4.09.

*N,N-Diethyl-3-cyclopropylmethoxy-4-difluoromethoxybenzamide (**10p**).* Yield: 92%. ^{1}H NMR (400 MHz, $CDCl_3$) δ 7.16 (d, J = 8.4 Hz, 1H), 6.98 (d, J = 2 Hz, 1H), 6.92 (dd, J = 8.0 Hz, 1H), 6.64 (t, J = 75.4 Hz, 1H), 3.88 (d, J = 7.2 Hz, 2H), 3.50−3.25 (m, 4H), 1.33−1.27 (m, 1H), 1.19 (s, 6H), 0.67−0.62 (m, 2H), 0.37−0.33 (m, 2H). ^{13}C NMR (100 MHz, $CDCl_3$) δ 170.3, 150.6, 141.0, 135.5, 122.4, 118.9, 118.7 (−CHF_2), 116.1 (−CHF_2), 113.5 (−CHF_2), 113.0, 74.0, 13.5, 10.1, 3.2. ESI-MS (m/z): 314.9 ([M + H]$^+$). Anal. Calcd for $C_{16}H_{21}F_2NO_3$: C, 61.33; H, 6.76; N, 4.47. Found: C, 61.56; H, 6.92; N, 4.71.

Pharmacology. *In Vitro Assay of Compounds for the Inhibition of PDEs. Materials.* Compounds **10a**−**p** were dissolved in DMSO and stored as stock solutions (100 mM) at −20 °C. For experimental use, all the compounds were prepared from stock solutions, diluted with growth medium, and used immediately. Fluorescamine (FAM)−cyclic-3′,5′-AMP and IMAP binding reagent were purchased from Molecular Devices Inc. PDE4CAT and other PDEs were purchased from SB Drug Discovery Inc. and BPS Bioscience Inc., respectively.

Assay. A standard PDE assay was conducted. All of our assays used a substrate concentration below the K_m determined for each enzyme such that K_i = IC_{50}. Our assay utilized IMAP technology (Molecular Devices), which is based on high-affinity binding of phosphate by immobilized metal coordination complexes on nanoparticles. The binding reagent complexes with phosphate groups on nucleotide monophosphate were generated from cyclic nucleotides (cAMP/cGMP) through PDEs. Binding induces a change in the rate of molecular motion of the phosphate-bearing molecule and results in increased fluorescence polarization observed for the fluorescent label attached to the substrate. These assays were carried out as described previously.[51] All enzymatic reactions were conducted at 25 °C for 60 min. The 50 μL reaction mixture contains 40 mM MOPS, pH 7.5, 0.5 mM EDTA, 15 mM $MgCl_2$, 0.15 mg/mL BSA, 1 mM DTT, 0.05% Proclin 200, 15 ng/mL PDE4CAT, and 100 nM FAM-cyclic-3′,5′-AMP. The compounds were diluted in 10% DMSO, and 5 μL of the dilution was added to a 50 μL reaction mixture to obtain a 1% final concentration of DMSO in all the reactions. The reaction mixture was incubated at 25 °C for 1 h followed by addition of 100 μL of diluted binding agent to each well, and then incubated at 25 °C for 1 h with slow shaking. The fluorescence polarization of the sample used an excitation filter of 360 nm and an emission filter of 480 nm. The percentage of inhibition was calculated using the following formula: % activity = $[(FP_{drug} - FP_{control})/(FP_{enzyme} - FP_{control})] \times 100\%$. The IC_{50} values were calculated using nonlinear regression with normalized dose−response fit using Prism GraphPad software.

Western Blotting Analysis. BV-2 cells were obtained from Sun Yat-sen University (Guangzhou, China). Cells were plated at a density of 1 × 10^6 in 6-well microculture plates and grown at 37 °C, with 90% humidity and 5% CO_2 in DMEM with high glucose supplemented with 10% FBS and antibiotics. Twenty-four hours later, the original medium was removed, DMEM medium without serum (900 μL) was added, and the culture was incubated for 1 h, then different concentrations (50, 200, and 800 μM) of drugs (100 μL) were added, respectively. After 1 h, LPS (10 μg/mL, 111 μL) was added to drug-treated and LPS-control group. After 24 h incubation, the cells

DOI: 10.1021/acschemneuro.6b00271
ACS Chem. Neurosci. XXXX, XXX, XXX−XXX

were lysed and centrifuged, and the supernatant was collected to analyze the total protein using BCA assay kit. Samples were then separated by electrophoresis in 10−15% sodium dodecyl sulfate-polyacrylamide gels and transferred to poly(vinylidene difluoride) (PVDF) membranes. Membranes were incubated with 5% nonfat milk for 2 h at room temperature to block nonspecific bindings. After washing, membranes were incubated with the respective primary antibodies for rabbit anti-TNF-α (1:1000, Millipore, USA), anti-iNOS (1:1000, CST, Danvers, MA, USA), and anti-COX-2 (1:1000, CST, Danvers, MA, USA) at 4 °C overnight. The membranes were washed three times with TBST and incubated with secondary antibodies (1:5000, Fdbio science, China) for 1 h at room temperature. After washing three times with TBST, the bands were detected using enhanced chemiluminescence (ECL), visualized using a Kodak Digital Science ID, and quantified by the software ImageJ 6.0.

In Vivo Antidepressant Behavioral Evaluation of Compound ***10j****. Animals.* Male C57BL/6 mice aged 7−9 weeks and weighing 18−22 g were purchased from the Laboratory Animal Centre of Southern Medical University (Guangzhou, China). After acclimation for 1 week, the animals were used for the experiments. The animals were housed at 22 ± 1 °C under a 12:12 h light/dark cycle, with free access to standard food pellets and water. The experiments were conducted in accordance with the National Institutes of Health Guide for the Care and Use of Laboratory Animals. The experiments were approved by the Laboratory Animal Ethics Committee of Southern Medical University.

Materials. Compound **10j** was dissolved in a small amount of DMSO and then in 0.9% saline. DMSO (5%) in saline (0.9%) was used as a control. Drugs were administered by injecting the doses indicated. Male C57BL/6 mice were randomly divided into five groups (n = 8/group): vehicle (DMSO in 0.9% saline), compound **10j**-treated (0.2, 0.4, and 0.8 mg/kg), and rolipram-treated (0.5 mg/kg, positive control) groups. All experiments were started at 8:00 a.m. and are briefly detailed here.

Mice were administered treatments by intraperitoneal injection. Vehicle group was treated with solvents, while the other treatment groups were treated with the corresponding dose of compound **10j** or rolipram. After 0.5 h, open field test, TST, and FST were conducted.

Open Field Test.[52] Each animal was individually placed in the center of the open field arena (60 × 60 × 35 cm^3). The ambulation scores (number of squares crossed) and rears (with both front paws raised from the floor) were recorded over a 5 min period with a video camera placed above the apparatus. In order to avoid interference, the apparatus was sprayed with alcohol and wiped thoroughly to eliminate residual odor after each test.

Tail-Suspension Test (TST).[30] Each individual mouse was suspended 40 cm above the table top using adhesive tape placed approximately 1.5 cm from the tip of the tail. The duration of immobility was recorded for 6 min. Immobility was defined as the absence of all movement except respiration.

Forced-Swim Test (FST).[30] Mice were placed individually in a plastic cylinder (45 cm high × 20 cm diameter) filled with water (23−24 °C; 28 cm in depth), allowing free swimming. The duration of the test was 6 min. The behavior was evaluated by a trained investigator. Immobility was defined as the absence of all movement except for minor movements required for the mouse to keep its head above the surface.

Statistical Analysis. Statistical analysis was performed and figures were produced using Prism 5 for Windows (Graph-Pad Software, Inc., San Diego, CA, USA). Data were expressed as mean ± standard error of mean (SEM). All data were analyzed using one-way analysis of variance (ANOVA) followed by Bonferroni's Multiple Comparison tests for post hoc analyses between the groups, with the exception of MWM acquisition trial data, which were analyzed by two-way repeated-measures ANOVA. Results were considered statistically significant when $p < 0.05$.

Ketamine/Xylazine-Induced Anesthesia. According to a previously described method,[50,53] which was modified by us, compound **10j** (FCPR03) (0.5, 1.0, and 1.5 mg/kg) or rolipram (0.5 mg/kg, a reference drug) was intragastrically administrated into 8−12-week-old male C57BL/6 mice 15 min prior to an intraperitoneal injection of ketamine (70 mg/kg)/xylazine (10 mg/kg). The vehicle (control) for FCPR03 or rolipram was a mixture of 5% DMSO, 20% β-cyclodextrin, and 6% polyoxyethylene 8 stearate dissolved in saline. After loss of the righting reflex (righting reflex is defined as when an animal placed on its back spontaneously righted itself to a prone position), the duration of anesthesia was measured until return of righting reflex as the end point. It is a common method to estimate the emetic potential of PDE4 inhibitors in rodents that do not have a vomiting reflex.

Effects of Compound ***10j*** *on Emesis in Beagle Dogs. Materials.* Compound **10j** and rolipram were dissolved in aqueous solution of carboxymethylcellulose sodium (CMC-Na, 0.5%).

Assay. Eleven beagle dogs were randomly divided into three groups each time, vehicle group (aqueous solution of CMC-Na (0.5%)), compound **10j**-treated (0.8 mg/kg) group, and rolipram-treated (0.8 mg/kg) group. The dogs were dosed by oral route with a volume of 1 mL/kg. After oral dosing, the animals were monitored continuously for 3 h. The incidence rate of emesis (%, the number of animals showing emesis per number of animals tested at the respective dose) and the latency of emesis (min) were recorded.

Pharmacokinetics Analysis. Pharmacokinetic properties of compound **10j** were assessed by HDBioscieces and Medicilon Companies, Shanghai, China. Six male SD rats with body weight of 237−267 g were purchased from Shanghai SIPPR-BK LAB Animal Ltd., Shanghai, China, and used for the pharmacokinetic analysis of **10j**. Compound **10j** was dissolved in 5% DMSO, 40% PEG400, and 55% saline for intravenous administration (iv) and oral administration (po). Final dosages of 1 mg/kg (iv) and 5 mg/kg (po) of the formulated compounds was administrated in mouse and rat, and the blood samples were taken at various time points in 24 h. The concentration of the compound in blood was analyzed by LC−MS/MS (Shimadzu liquid chromatographic system and API4000 mass spectrometer, Applied Biosystems, Ontario, Canada).

Molecular Docking. Molecular docking was performed with Surflex-Dock program interfaced with Sybyl 7.3. The programs adopted an empirical scoring function and a patented search engine.[54,55] Ligand was docked into the corresponding protein-binding site guided by protomol, which is an idealized representation of a ligand that makes every potential interaction with the binding site. In this work, the protomol was established by ligand from the crystal structure of PDE4D (PDB entry 3G4K).[28] Docking was initiated by removing all ligands followed by addition of random hydrogen atoms. The receptor structure was minimized in 10 000 cycles with Powell method in Sybyl 7.3. All the compounds were constructed using a sketch molecular module. Hydrogen and Gasteiger−Hückel charges were added to each molecule. Water molecules conserved in PDE4D structures deposited into PDB were considered for calculations. Their geometries were optimized by conjugate gradient method in TRIPOS force field. The energy convergence criterion was 0.001 kcal/mol. Default values were selected to complete this work except that the threshold was 1 when the protomol was generated.

To validate docking reliability, the cocrystallized ligand (rolipram) was removed from the active site and docked back into the known binding pocket. The root-mean-square deviation (RMSD) between the predicted conformation and the actual conformation from the crystal structure of ligand was 1.29 Å, which was smaller than the resolution of X-ray crystallography 1.95 Å.[28] Thus, the parameters set for this Surflex-dock simulation successfully reproduced the ligand-binding motif in the X-ray structure and were extrapolated to predict the binding conformations of the synthesized inhibitors.

■ ASSOCIATED CONTENT

Supporting Information

The Supporting Information is available free of charge on the ACS Publications website at DOI: 10.1021/acschemneuro.6b00271.

^{1}H and ^{13}C NMR spectra of compounds **10a−p** (PDF)

DOI: 10.1021/acschemneuro.6b00271
ACS Chem. Neurosci. XXXX, XXX, XXX−XXX

AUTHOR INFORMATION

Corresponding Authors

*Phone: +86 02061648235. Fax: +86 02061648236. E-mail address: zhouzz@smu.edu.cn (Z.-Z Zhou).
*E-mail address: yxmjp@sina.com (X.-M. Yang).
*E-mail address: jpx@smu.edu.cn (J.-P. Xu).

Author Contributions

The manuscript was written through contributions of all authors. All authors have given approval to the final version of the manuscript.

Funding

This work was financially supported by the Foundation for Guangdong Distinguished Young Teachers in Higher Education of China (No. C1032190) and the Science and Technology Program of Guangdong Province of China (No. 2016A020217008) awarded to Z.Z.Z, the National Science and Technology Major Projects of China for "Major New Drug Innovation and Development" (No. 2012ZX09J1211003C), NSFC-Guangdong Joint Fund (No. U1032006), and the National Natural Science Foundation of China (No. 81373384) awarded to J.P.X.

Notes

The authors declare no competing financial interest.

ABBREVIATIONS

BSA, bovine serum albumin; cAMP, cyclic adenosine monophosphate; cGMP, cyclic guanosine monophosphate; COX-2, cyclooxygenase-2; DMEM, Dulbecco's modified Eagle's medium; DMSO, dimethyl sulfoxide; DTT, dithiothreitol; EDTA, ethylenediaminetetraacetic acid; ESI, electrospray ionization; FAM, fluorescamine; FBS, fetal bovine serum; FST, forced swimming test; iNOS, inducible nitric oxide synthase; LC−MS, liquid chromatography−mass spectrometry; LPSs, lipopolysaccharides; DCM, dichloromethane; MOPS, 3-(*N*-morpholino)propanesulfonic acid; NMR, nuclear magnetic resonance; PDEs, phosphodiesterases; PDE4, phosphodiesterase 4; PDE4CAT, the core catalytic domains of human PDE4; $SOCl_2$, sulfurous dichloride; TBST, Tris-buffered saline with Tween 20; TEA, triethylamine; TLC, thin-layer chromatography; TNF-α, tumor necrosis factor-alpha; TST, tail suspension test

REFERENCES

(1) Maes, M., Yirmyia, R., Noraberg, J., Brene, S., Hibbeln, J., Perini, G., Kubera, M., Bob, P., Lerer, B., and Maj, M. (2009) The inflammatory & neurodegenerative (I&ND) hypothesis of depression: leads for future research and new drug developments in depression. *Metab. Brain Dis. 24*, 27−53.

(2) Pehrson, A. L., Leiser, S. C., Gulinello, M., Dale, E., Li, Y., Waller, J. A., and Sanchez, C. (2015) Treatment of cognitive dysfunction in major depressive disorder-a review of the preclinical evidence for efficacy of selective serotonin reuptake inhibitors, serotonin-norepinephrine reuptake inhibitors and the multimodal-acting antidepressant vortioxetine. *Eur. J. Pharmacol. 753*, 19−31.

(3) Belmaker, R. H., and Agam, G. (2008) Major depressive disorder. *N. Engl. J. Med. 358*, 55−68.

(4) Rosenblat, J. D., Cha, D. S., Mansur, R. B., and McIntyre, R. S. (2014) Inflamed moods: a review of the interactions between inflammation and mood disorders. *Prog. Neuro-Psychopharmacol. Biol. Psychiatry 53*, 23−34.

(5) Grosse, L., Carvalho, L. A., Wijkhuijs, A. J., Bellingrath, S., Ruland, T., Ambree, O., Alferink, J., Ehring, T., Drexhage, H. A., and Arolt, V. (2015) Clinical characteristics of inflammation-associated depression: Monocyte gene expression is age-related in major depressive disorder. *Brain, Behav., Immun. 44*, 48−56.

(6) Raison, C. L., Rutherford, R. E., Woolwine, B. J., Shuo, C., Schettler, P., Drake, D. F., Haroon, E., and Miller, A. H. (2013) A randomized controlled trial of the tumor necrosis factor antagonist infliximab for treatment-resistant depression: the role of baseline inflammatory biomarkers. *JAMA Psychiatry 70*, 31−41.

(7) Muller, N., Schwarz, M. J., Dehning, S., Douhe, A., Cerovecki, A., Goldstein-Muller, B., Spellmann, I., Hetzel, G., Maino, K., Kleindienst, N., Möller, H. J., Arolt, V., and Riedel, M. (2006) The cyclooxygenase-2 inhibitor celecoxib has therapeutic effects in major depression: results of a double-blind, randomized, placebo controlled, add-on pilot study to reboxetine. *Mol. Psychiatry 11*, 680−684.

(8) Hansen, R. T., III, and Zhang, H.-T. (2015) Phosphodiesterase-4 modulation as a potential therapeutic for cognitive loss in pathological and non-pathological aging: possibilities and pitfalls. *Curr. Pharm. Des. 21*, 291−302.

(9) Omori, K., and Kotera, J. (2007) Overview of PDEs and their regulation. *Circ. Res. 100*, 309−327.

(10) Keravis, T., and Lugnier, C. (2012) Cyclic nucleotide phosphodiesterase (PDE) isozymes as targets of the intracellular signalling network: benefits of PDE inhibitors in various diseases and perspectives for future therapeutic developments. *Br. J. Pharmacol. 165*, 1288−1305.

(11) Zhang, H.-T. (2009) Cyclic AMP-specific phosphodiesterase-4 as a target for the development of antidepressant drugs. *Curr. Pharm. Des. 15*, 1688−1698.

(12) Peng, S., Sun, H., Zhang, X., Liu, G., and Wang, G. (2014) Effects of Selective Phosphodiesterases-4 Inhibitors on Learning and Memory: A Review of Recent Research. *Cell Biochem. Biophys. 70*, 83−85.

(13) Sierksma, A. S. R., van den Hove, D. L. A., Pfau, F., Philippens, M., Bruno, O., Fedele, E., Ricciarelli, R., Steinbusch, H. W. M., Vanmierlo, T., and Prickaerts, J. (2014) Improvement of spatial memory function in APPswe/PS1dE9 mice after chronic inhibition of phosphodiesterase type 4D. *Neuropharmacology 77*, 120−130.

(14) Martinez, A., and Gil, C. (2014) cAMP-specific phosphodiesterase inhibitors: promising drugs for inflammatory and neurological diseases. *Expert Opin. Ther. Pat. 24*, 1311−1321.

(15) Zhang, H. T., Huang, Y., Masood, A., Stolinski, L. R., Li, Y., Zhang, L., Dlaboga, D., Jin, S. L., Conti, M., and O'Donnell, J. M. (2008) Anxiogenic-like behavioral phenotype of mice deficient in phosphodiesterase 4B (PDE4B). *Neuropsychopharmacology 33*, 1611−1623.

(16) Siuciak, J. A., McCarthy, S. A., Chapin, D. S., and Martin, A. N. (2008) Behavioral and neurochemical characterization of mice deficient in the phosphodiesterase-4B (PDE4B) enzyme. *Psychopharmacology (Berlin, Ger.) 197*, 115−126.

(17) Schaefer, T. L., Braun, A. A., Amos-Kroohs, R. M., Williams, M. T., Ostertag, E., and Vorhees, C. V. (2012) A new model of Pde4d deficiency: genetic knock-down of PDE4D enzyme in rats produces an antidepressant phenotype without spatial cognitive effects. *Genes, Brain Behav. 11*, 614−622.

(18) Zhang, H.-T., Huang, Y., Jin, S. L. C., Frith, S. A., Suvarna, N., Conti, M., and O'Donnell, J. M. (2002) Antidepressant-like Profile and Reduced Sensitivity to Rolipram in Mice Deficient in the PDE4D Phosphodiesterase Enzyme. *Neuropsychopharmacology 27*, 587−595.

(19) Ji, Q., Di, Y., He, X., Liu, Q., Liu, J., Li, W., and Zhang, L. (2016) Intrathecal injection of phosphodiesterase 4B-specific siRNA attenuates neuropathic pain in rats with L5 spinal nerve ligation. *Mol. Med. Rep. 13*, 1914−1922.

(20) Wang, Z.-Z., Zhang, Y., Liu, Y.-Q., Zhao, N., Zhang, Y.-Z., Yuan, L., An, L., Li, J., Wang, X.-Y., Qin, J.-J., Wilson, S. P., O'Donnell, J. M., Zhang, H.-T., and Li, Y.-F. (2013) RNA interference-mediated phosphodiesterase 4D splice variants knock-down in the prefrontal cortex produces antidepressant-like and cognition-enhancing effects. *Br. J. Pharmacol. 168*, 1001−1014.

(21) Plattner, F., Hayashi, K., Hernandez, A., Benavides, D. R., Tassin, T. C., Tan, C., Day, J., Fina, M. W., Yuen, E. Y., Yan, Z.,

DOI: 10.1021/acschemneuro.6b00271
ACS Chem. Neurosci. XXXX, XXX, XXX−XXX

Goldberg, M. S., Nairn, A. C., Greengard, P., Nestler, E. J., Taussig, R., Nishi, A., Houslay, M. D., and Bibb, J. A. (2015) The role of ventral striatal cAMP signaling in stress-induced behaviors. *Nat. Neurosci. 18*, 1094−1110.

(22) Tashkin, D. P. (2014) Roflumilast: the new orally active, selective phophodiesterase-4 inhibitor, for the treatment of COPD. *Expert Opin. Pharmacother. 15*, 85−96.

(23) Abdulrahim, H., Thistleton, S., Adebajo, A. O., Shaw, T., Edwards, C., and Wells, A. (2015) Apremilast: a PDE4 inhibitor for the treatment of psoriatic arthritis. *Expert Opin. Pharmacother. 16*, 1099−1108.

(24) Norman, T. R., Judd, F. K., and Burrows, G. D. (1992) New pharmacological approaches to the management of depression: from theory to clinical practice. *Aust. N. Z. J. Psychiatry 26*, 73−81.

(25) Cheng, Y.-F., Wang, C., Lin, H.-B., Li, Y.-F., Huang, Y., Xu, J.-P., and Zhang, H.-T. (2010) Inhibition of phosphodiesterase-4 reverses memory deficits produced by Abeta25−35 or Abeta1−40 peptide in rats. *Psychopharmacology (Berl) 212*, 181−191.

(26) Li, L.-X., Cheng, Y.-F., Lin, H.-B., Wang, C., Xu, J.-P., and Zhang, H.-T. (2011) Prevention of cerebral ischemia-induced memory deficits by inhibition of phosphodiesterase-4 in rats. *Metab. Brain Dis. 26*, 37−47.

(27) Wang, C., Yang, X.-M., Zhuo, Y.-Y., Zhou, H., Lin, H.-B., Cheng, Y.-F., Xu, J.-P., and Zhang, H.-T. (2012) The phosphodiesterase-4 inhibitor rolipram reverses Abeta-induced cognitive impairment and neuroinflammatory and apoptotic responses in rats. *Int. J. Neuropsychopharmacol. 15*, 749−766.

(28) Burgin, A. B., Magnusson, O. T., Singh, J., Witte, P., Staker, B. L., Bjornsson, J. M., Thorsteinsdottir, M., Hrafnsdottir, S., Hagen, T., Kiselyov, A. S., Stewart, L. J., and Gurney, M. E. (2010) Design of phosphodiesterase 4D (PDE4D) allosteric modulators for enhancing cognition with improved safety. *Nat. Biotechnol. 28*, 63−70.

(29) Bruno, O., Fedele, E., Prickaerts, J., Parker, L. A., Canepa, E., Brullo, C., Cavallero, A., Gardella, E., Balbi, A., Domenicotti, C., Bollen, E., Gijselaers, H. J. M., Vanmierlo, T., Erb, K., Limebeer, C. L., Argellati, F., Marinari, U. M., Pronzato, M. A., and Ricciarelli, R. (2011) GEBR-7b, a novel PDE4D selective inhibitor that improves memory in rodents at non-emetic doses. *Br. J. Pharmacol. 164*, 2054−2063.

(30) Zhang, M. Z., Zhou, Z. Z., Yuan, X., Cheng, Y. F., Bi, B. T., Gong, M. F., Chen, Y. P., and Xu, J. P. (2013) Chlorbipram: a novel PDE4 inhibitor with improved safety as a potential antidepressant and cognitive enhancer. *Eur. J. Pharmacol. 721*, 56−63.

(31) Zhou, Z.-Z., Ge, B.-C., Chen, Y.-F., Shi, X.-D., Yang, X.-M., and Xu, J.-P. (2015) Catecholic amides as potential selective phosphodiesterase 4D inhibitors: Design, synthesis, pharmacological evaluation and structure−activity relationships. *Bioorg. Med. Chem. 23*, 7332−7339.

(32) Zhou, Z.-Z., Ge, B.-C., Zhong, Q.-P., Huang, C., Cheng, Y.-F., Yang, X.-M., Wang, H.-T., and Xu, J.-P. (2016) Development of highly potent phosphodiesterase 4 inhibitors with anti-neuroinflammation potential: Design, synthesis, and structure-activity relationship study of catecholamides bearing aromatic rings. *Eur. J. Med. Chem. 124*, 372.

(33) Zheng, S., Kaur, G., Wang, H., Li, M., Macnaughtan, M., Yang, X., Reid, S., Prestegard, J., Wang, B., and Ke, H. (2008) Design, synthesis, and structure-activity relationship, molecular modeling, and NMR studies of a series of phenyl alkyl ketones as highly potent and selective phosphodiesterase-4 inhibitors. *J. Med. Chem. 51*, 7673−7688.

(34) Card, G. L., England, B. P., Suzuki, Y., Fong, D., Powell, B., Lee, B., Luu, C., Tabrizizad, M., Gillette, S., Ibrahim, P. N., Artis, D. R., Bollag, G., Milburn, M. V., Kim, S.-H., Schlessinger, J., and Zhang, K. Y. J. (2004) Structural Basis for the Activity of Drugs that Inhibit Phosphodiesterases. *Structure 12*, 2233−2247.

(35) Wang, H., Robinson, H., and Ke, H. (2007) The molecular basis for different recognition of substrates by phosphodiesterase families 4 and 10. *J. Mol. Biol. 371*, 302−327.

(36) Zhang, K. Y., Card, G. L., Suzuki, Y., Artis, D. R., Fong, D., Gillette, S., Hsieh, D., Neiman, J., West, B. L., Zhang, C., Milburn, M. V., Kim, S. H., Schlessinger, J., and Bollag, G. (2004) A glutamine switch mechanism for nucleotide selectivity by phosphodiesterases. *Mol. Cell 15*, 279−286.

(37) Yang, G.-F., Lu, H.-T., Xiong, Y., and Zhan, C.-G. (2006) Understanding the structure−activity and structure−selectivity correlation of cyclic guanine derivatives as phosphodiesterase-5 inhibitors by molecular docking, CoMFA and CoMSIA analyses. *Bioorg. Med. Chem. 14*, 1462−1473.

(38) Xiong, Y., Lu, H.-T., Li, Y., Yang, G.-F., and Zhan, C.-G. (2006) Characterization of a Catalytic Ligand Bridging Metal Ions in Phosphodiesterases 4 and 5 by Molecular Dynamics Simulations and Hybrid Quantum Mechanical/Molecular Mechanical Calculations. *Biophys. J. 91*, 1858−1867.

(39) Hagen, T. J., Mo, X., Burgin, A. B., Fox, D., Zhang, Z., and Gurney, M. E. (2014) Discovery of triazines as selective PDE4B versus PDE4D inhibitors. *Bioorg. Med. Chem. Lett. 24*, 4031−4034.

(40) Nankervis, J. L., Feil, S. C., Hancock, N. C., Zheng, Z., Ng, H.-L., Morton, C. J., Holien, J. K., Ho, P. W. M., Frazzetto, M. M., Jennings, I. G., Manallack, D. T., Martin, T. J., Thompson, P. E., and Parker, M. W. (2011) Thiophene inhibitors of PDE4: Crystal structures show a second binding mode at the catalytic domain of PDE4D2. *Bioorg. Med. Chem. Lett. 21*, 7089−7093.

(41) van Dooren, F. E., Schram, M. T., Schalkwijk, C. G., Stehouwer, C. D., Henry, R. M., Dagnelie, P. C., Schaper, N. C., van der Kallen, C. J., Koster, A., Sep, S. J., Denollet, J., Verhey, F. R., and Pouwer, F. (2016) Associations of low grade inflammation and endothelial dysfunction with depression - The Maastricht Study. *Brain, Behav., Immun. 56*, 390−396.

(42) Boorman, E., Zajkowska, Z., Ahmed, R., Pariante, C. M., and Zunszain, P. A. (2016) Crosstalk between endocannabinoid and immune systems: a potential dysregulation in depression? *Psychopharmacology 233*, 1591−1604.

(43) Kelley, K. W., O'Connor, J. C., Lawson, M. A., Dantzer, R., Rodriguez-Zas, S. L., and McCusker, R. H. (2013) Aging leads to prolonged duration of inflammation-induced depression-like behavior caused by Bacillus Calmette-Guerin. *Brain, Behav., Immun. 32*, 63−69.

(44) Fox, D., III, Burgin, A. B., and Gurney, M. E. (2014) Structural basis for the design of selective phosphodiesterase 4B inhibitors. *Cell. Signalling 26*, 657−663.

(45) Zhou, D., Jin, H., Lin, H. B., Yang, X. M., Cheng, Y. F., Deng, F. J., and Xu, J. P. (2010) Antidepressant effect of the extracts from Fructus Akebiae. *Pharmacol., Biochem. Behav. 94*, 488−495.

(46) Villetti, G., Carnini, C., Battipaglia, L., Preynat, L., Bolzoni, P. T., Bassani, F., Caruso, P., Bergamaschi, M., Pisano, A. R., Puviani, V., Stellari, F. F., Cenacchi, V., Volta, R., Bertacche, V., Mileo, V., Bagnacani, V., Moretti, E., Puccini, P., Catinella, S., Facchinetti, F., Sala, A., and Civelli, M. (2015) CHF6001 II: A Novel Phosphodiesterase 4 Inhibitor, Suitable for Topical Pulmonary Administration-In Vivo Preclinical Pharmacology Profile Defines a Potent Anti-Inflammatory Compound with a Wide Therapeutic Window. *J. Pharmacol. Exp. Ther. 352*, 568−578.

(47) Vanmierlo, T., Creemers, P., Akkerman, S., van Duinen, M., Sambeth, A., De Vry, J., Uz, T., Blokland, A., and Prickaerts, J. (2016) The PDE4 inhibitor roflumilast improves memory in rodents at non-emetic doses. *Behav. Brain Res. 303*, 26−33.

(48) Kenward, H., Pelligand, L., and Elliott, J. (2014) Assessment of low-dose cisplatin as a model of nausea and emesis in beagle dogs, potential for repeated administration. *Exp. Brain Res. 232*, 2685−2697.

(49) Gobejishvili, L., Barve, S., Joshi-Barve, S., and McClain, C. (2008) Enhanced PDE4B expression augments LPS-inducible TNF expression in ethanol-primed monocytes: relevance to alcoholic liver disease. *Am. J. Physiol. 295*, G718−G724.

(50) Robichaud, A., Stamatiou, P. B., Jin, S. L., Lachance, N., MacDonald, D., Laliberte, F., Liu, S., Huang, Z., Conti, M., and Chan, C. C. (2002) Deletion of phosphodiesterase 4D in mice shortens alpha(2)-adrenoceptor-mediated anesthesia, a behavioral correlate of emesis. *J. Clin. Invest. 110*, 1045−1052.

(51) Huang, W., Zhang, Y., and Sportsman, J. R. (2002) A fluorescence polarization assay for cyclic nucleotide phosphodiesterases. *J. Biomol. Screening 7*, 215−222.

DOI: 10.1021/acschemneuro.6b00271
ACS Chem. Neurosci. XXXX, XXX, XXX−XXX

(52) Zhang, C., Cheng, Y., Wang, H., Wang, C., Wilson, S. P., Xu, J., and Zhang, H.-T. (2014) RNA interference-mediated knockdown of long-form phosphodiesterase-4D (PDE4D) enzyme reverses amyloid-beta42-induced memory deficits in mice. *J. Alzheimers Dis. 38*, 269−280.
(53) Robichaud, A., Savoie, C., Stamatiou, P. B., Lachance, N., Jolicoeur, P., Rasori, R., and Chan, C. C. (2002) Assessing the emetic potential of PDE4 inhibitors in rats. *Br. J. Pharmacol. 135*, 113−118.
(54) Jain, A. N. (2007) Surflex-Dock 2.1: robust performance from ligand energetic modeling, ring flexibility, and knowledge-based search. *J. Comput.-Aided Mol. Des. 21*, 281−306.
(55) Jain, A. N. (2003) Surflex: fully automatic flexible molecular docking using a molecular similarity-based search engine. *J. Med. Chem. 46*, 499−511.

DOI: 10.1021/acschemneuro.6b00271
ACS Chem. Neurosci. XXXX, XXX, XXX−XXX